THE ORIGIN OF MERCURY'S OLDEST SURFACES AND THE NATURE OF INTERCRATER PLAINS RESURFACING.

Brett W. Denevi[1] Carolyn M. Ernst[1], Louise M. Prockter[1], Mark S. Robinson[2], Paul. D. Spudis[3], Rachel L. Klima[1], Scott L. Murchie[1], Sean C. Solomon[4,5], Jennifer L. Whitten[6], Reinhold Z. Povilaitis[2], and Mallory J. Kinczyk[1], [1]The Johns Hopkins University Applied Physics Laboratory, Laurel, MD 20723, USA, [2]School of Earth and Space Exploration, Arizona State University, Tempe, AZ 85287, USA, [3]Lunar and Planetary Institute, Houston, TX 77058, USA, [4]Lamont-Doherty Earth Observatory, Columbia University, Palisades, NY 10964, USA, [5]Department of Terrestrial Magnetism, Carnegie Institution of Washington, Washington, DC 20015, USA, [6]Center for Earth and Planetary Studies, Smithsonian Institution, Washington, DC 20560, USA.

Introduction: The intercrater plains are the most areally extensive unit on Mercury and interpreted to be the oldest geological unit on the planet [1–4]. Despite the fact that the intercrater plains have been heavily modified by impacts, they are not as heavily cratered as might be expected—the density of superposed craters with large diameters is substantially lower than that of the lunar highlands (Fig. 1). The relatively low density of craters >20 km in diameter on Mercury was well established for terrain viewed by Mariner 10 [e.g., 5,6] and is now confirmed as a global phenomenon [7–9], in contrast to the expectation that approximately two to three times as many craters in this size range formed on Mercury as on the Moon [9–11]. On the basis of these comparatively low crater densities, it is inferred that Mercury's oldest surfaces along with a substantial portion of the earliest crater population was resurfaced, and the intercrater plains observed today are the result of that resurfacing. Areas that did not suffer complete resurfacing may represent the oldest crustal materials still exposed, and thus are key to understanding the origin of Mercury's early crust.

Mercury's Oldest Surfaces: We examined an area south of the Caloris basin that represents the broadest expanse of terrain with the greatest $N(65)$ values, where $N(D)$ is the number of craters with diameter ≥ D (in km) per million km^2 (Fig. 1). The $N(65)$ crater density of this area is similar to the values for the lunar highlands (Fig. 1), suggesting that both areas may have reached saturation equilibrium [7,12], despite the fact that the $N(20)$ values are substantially below those of the lunar highlands. Evidence for partial resurfacing is observed in images of the region: patchy deposits of smooth plains fill crater floors and other topographic lows (Fig. 2), and these deposits are likely responsible for the removal of small craters and the low $N(20)$ values. Their sporadic distribution and distance from both Caloris and Rembrandt (3–4 basin radii from the rim) suggests that these smooth plains could be of impact ejecta origin, similar to the smooth plains around the lunar Orientale basin [13]. If this is the case, their color contrast (moderately higher in reflectance, steeper spectral slope) with surrounding terrain indicates they likely contain substantial primary basin ejecta. Alternately, these smooth plains may be volcanic in origin. Areas not affected by smooth plains correspond to a regional expanse of old low-reflectance material (LRM) [14–17], which has been interpreted as rich in graphite on the basis of its spectral reflectance and neutron absorption properties [16,18]. LRM is concentrated in crater ejecta in this region (Fig. 2).

The stratigraphy of the region, i.e., that all material excavated from depth is either comparable to or lower in reflectance than the surrounding terrain, is in contrast to other regions where both low- and high-reflectance materials were excavated from depth (see next section). These observations, combined with the high $N(65)$ crater density, suggest this may be a region where early crust escaped wholesale resurfacing and remains exposed at the surface, albeit in a heavily gardened form. The LRM seen concentrated in crater ejecta may have originally comprised the surface in this area but is now found beneath a mixed regolith with a reflectance that has been modestly raised by mixing

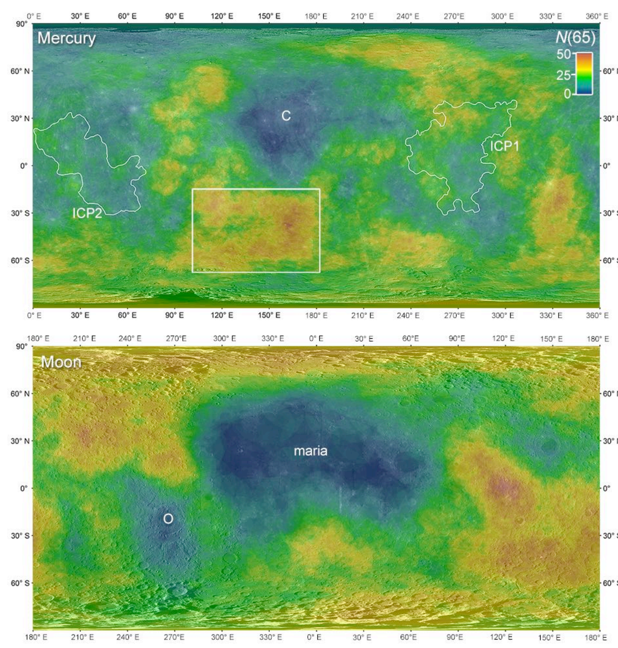

Fig. 1. The number of craters ≥65 km in diameter per million km^2, $N(65)$, for Mercury (top) and the Moon (bottom); color scale applies to both panels. Two regions of intercrater plains on Mercury are outlined (ICP1, 2), and the white box indicates a heavily cratered region south of Caloris (C). For the Moon, nearside maria and the Orientale (O) basin are indicated. Crater density derived from Fassett et al. [7] and Head et al. [19].

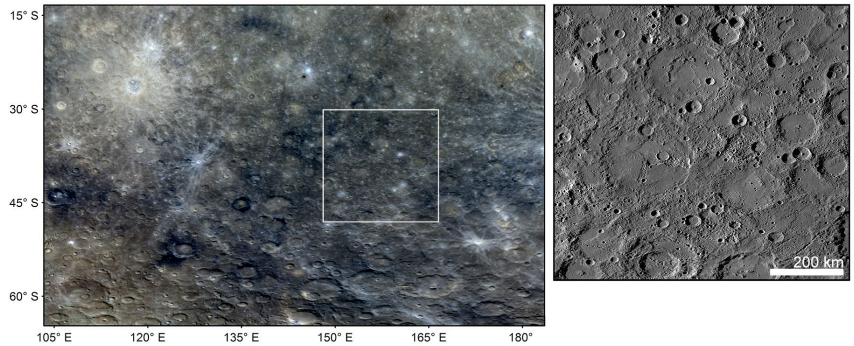

Fig. 2. Heavily cratered region of Fig. 1. A regional LRM deposit (left) covers much of the area (1000, 750, and 430 nm in red, green, and blue). The area in the white box is seen at right; large craters are abundant with patchy deposits of smooth plains.

from impacts of all sizes, but particularly basin-sized events. In addition to the two adjacent Calorian basins, eight basins are found near the margins of this region. Here an approximate analogy may be the lunar highlands, where pure anorthosite (thought to represent the original magma ocean flotation crust) is found beneath a more mafic megaregolith of mixed local material and basin ejecta and is exposed mainly within large craters and basins [e.g., 20]. However, on Mercury, at least in this region, the early crust had low reflectance and may be rich in graphite.

Intercrater Plains Resurfacing: Both impact and volcanic origins have been proposed for the formation of the intercrater plains. Both processes can bury preexisting impact craters and produce plains deposits, either by ballistic sedimentation [21] or effusive volcanism [e.g., 22]. It is unlikely that basin ejecta alone produced Mercury's near-global resurfacing. The large volume of intercrater plains could be explained if Mercury had more impact basins than the Moon [23], but the observed density of basins >300 km diameter is lower on Mercury than the Moon [24], though it is almost certain that there is a population of basins that is no longer recognizable. The higher impact velocities on Mercury lead to a larger volume of melt for a given size impact [e.g., 25] and a more fluid-like behavior for its ejecta, meaning that a larger fraction of the surface is likely affected per basin (although this effect would be mitigated by the more restricted ballistic range of ejecta on Mercury [25]). Still, the large thicknesses and vast areal extent of some intercrater plains units with distinct color properties are inconsistent with an impact origin and suggest that volcanism contributed a substantial fraction of the intercrater plains.

We examined two intercrater plains regions (Fig. 1), and in each we find strong evidence for a volcanic origin of the plains. The first (ICP1) is a region of pre-Tolstojan intercrater plains that is not associated with any identified large basins. The second region (ICP2) is Tolstojan in age, and intercrater plains largely bury two degraded basins, each close to 1500 km in diameter. In both regions, the majority of craters expose high-reflectance material with a steep spectral slope, similar to the volcanic smooth plains within the Caloris basin. Some craters >100 km in diameter and smaller craters near the margins of each region expose LRM, and their depths of excavation imply that several kilometers of high-reflectance material overlie LRM. We interpret these intercrater plains as having formed from early episodes (>3.9 Ga) of flood volcanism.

Summary: The geology and stratigraphy of the three regions explored here is consistent with the idea that Mercury's early crust was enriched in graphite and low in reflectance, comparable to that of LRM [16,18,26]. The thickness of LRM deposits is not well constrained but at least locally is substantially greater [27,28] than the relatively small values predicted for a graphite flotation crust [26]. Thus if it existed, a graphite flotation crust must have been mixed early (as a result of multiple magmatic and impact events, if not during magma ocean solidification), and only remnants of this mixed, brecciated material remain. Volcanic material derived from partial melting of the mantle would be generally higher in reflectance than the early crust, as is observed for the intercrater and smooth plains. As LRM is often exposed from depths of several kilometers [27,28], this scenario implies substantial volcanism subsequent to the development of LRM as widespread crustal material, consistent with earlier inferences on the emplacement history of the crust [14] and the observations of two regions of intercrater plains reported here. Mercury's modern crust is heterogeneous, and further work to understand the color-stratigraphic relationships of regional units will aid in deciphering the global picture apart from regional effects of impacts and volcanism.

References: [1] Trask N.J. and Guest J.E. (1975) *JGR*, *80*, 2461. [2] Spudis P.D. and Guest J.E. (1988) in *Mercury,* Univ. Ariz. Press, 118. [3] Prockter L.M. et al. (2016), *LPS,* this mtg. [4] Whitten J.L. et al. (2014) *Icarus*, *241*, 97. [5] Murray B.C. et al. (1975) *JGR*, *80*, 2508. [6] Strom R.G. (1977) *Phys. Earth Planet. Inter.*, *15*, 156. [7] Fassett C.I. et al. (2011) *GRL*, *38*, L10202. [8] Strom R.G. et al. (2011) *PSS*, *59*, 1960. [9] Marchi S. et al. (2013) *Nature*, *499*, 59. [10] Le Feuvre M. and Wieczorek M.A. (2008) *Icarus*, *197*, 291. [11] Greenstreet S. et al. (2012) *Icarus*, *217*, 355. [12] Hartmann W.K. (1984) *Icarus*, *60*, 56. [13] Meyer H.M. et al. (2016) *Icarus*, in press. [14] Denevi B.W. et al. (2009) *Science*, *324*, 613. [15] Klima R.L. et al. (2016) *LPS*, *47*, 1195. [16] Murchie S.L. et al. (2015) *Icarus*, *254*, 287. [17] Robinson M.S. et al. (2008) *Science*, *321*, 66. [18] Peplowski P.N. et al. (2016) *Nature Geosci.*, in press. [19] Head J.W. et al. (2010) *Science*, *329*, 1504. [20] Hawke B.R. et al. (2003) *JGR*, *108*, 5050. [21] Oberbeck V.R. et al. (1975) *Moon*, *12*, 19. [22] Head J.W. et al. (2011) *Science*, *333*, 1853. [23] Wilhelms D.E. (1976) *Icarus*, *28*, 551. [24] Fassett C.I. et al. (2012) *JGR*, *117*, E00L08. [25] Gault D.E. et al. (1975) *JGR*, *80*, 2444. [26] Vander Kaaden K.E. and McCubbin F.M. (2015) *JGR Planets, 120*, 195. [27] Ernst C.M. et al. (2010) *Icarus*, *209*, 210. [28] Ernst C.M. et al. (2015) *Icarus*, *250*, 413.